Preparation and performance of novel flavonoid phenols-based biomass-modified phenol formaldehyde resins

Yuan Qin
School of Materials Science and Engineering, Jiangsu University
Fuliang Meng
Hangmo New Materials Group Co., Ltd.
Chunyu Xu
Research School of Polymeric Materials, Jiangsu University
Zhenguo Hu
School of Materials Science and Engineering, Jiangsu University
Yimiao Zhang
School of Materials Science and Engineering, Jiangsu University
Yufei Jia
School of Materials Science and Engineering, Jiangsu University
Songjun Li
Research School of Polymeric Materials, Jiangsu University
Xinhua Yuan (yuanxh@ujs.edu.cn)
School of Materials Science and Engineering, Jiangsu University

Research Article

Keywords: Biomass-modified PF resin, Naringenin, Daidzein, Sustainable materials, Resin matrices for friction composites

Posted Date: January 10th, 2023

DOI: https://doi.org/10.21203/rs.3.rs-2448640/v1

Additional Declarations: No competing interests reported.

Version of Record: A version of this preprint was published at Journal of Inorganic and Organometallic Polymers and Materials on March 28th, 2023. See the published version at https://doi.org/10.1007/s10904-023-02619-7.

Abstract

Low toxicity, environmentally friendly and sustainable bio-based phenol-formaldehyde (PF) resins are the primary factors and health goals that researchers need to consider when modifying PF resins. Two novel biomass-modified PF resins were synthesized using two flavonoid phenols of daidzein and naringenin with rigid backbone structures. The results show that compared with ordinary PF, the introduction of daidzein and naringenin during the synthesis of N-PF and D-PF can delay the curing reaction and results in higher curing peak temperatures. The appropriate substitution rate of daidzein and naringenin can improve the crosslinking degree, resulting in N-PF and D-PF with higher thermal stability, ablation resistance and mechanical properties. The highest carbon yield YC800 for N-PF is 59.81% (56.85%for PF-1), and the highest YC800 for D-PF is 64.39% (PF-2 with 58.15%). The maximum tensile strength and flexural strengths of N-PF are respective 33.86 MPa and 110.42 MPa (28.77 and 79.89 MPa for PF-1), and the maximum tensile strength and flexural strengths of D-PF are respective 35.61 MPa and 103.17 MPa (24.48 and 55.79 MPa for PF-2). The D-PF and N-PF resins modified and enhanced by daidzein and naringenin have lower friction coefficient and more excellent wear resistance than pure PF.

1 Introduction

Compared with epoxy resin and benzoxazine resin, phenolic -formaldehyde resin (PF) has been more widely and systematically researched and applied in the course of more than one hundred years of development, showing superior use value[1]. Due to its excellent properties, such as flame retardancy, excellent sound insulation, water and chemical resistance, and abrasion resistance[2], PF can be used as flame retardant materials[3], battery application related materials[4, 5], adhesives[6], friction braking materials[7], adsorption materials[8] and separation membrane materials[9, 10], aerospace materials[11], etc. in emerging fields.

Although PF has good application advantages, it still cannot meet people's demands for environment-friendly and low toxicity applications. PF has many limitations, such as the non-renewable resource properties and toxicity of synthetic raw materials[12], the brittleness caused by rigid aromatic units and methylene structures[13], etc. These defects directly restrict the application of PF. With the improvement of people's awareness of environmental protection, more and more attention has been paid to the non-recyclable and non-reusable characteristics of PF as raw materials[14], and the health and environmental problems caused by formaldehyde release. On the basis of reducing health and environmental problems, functional requirements, economical and environmentally friendly biomass PF has become the primary goal of researchers.

In recent years, functional and environmentally friendly green materials using biomass as raw materials, such as bio-based polyurethane[15, 16], bio-based benzoxazine resin[17–19], bio-based PF[20], and bio-based epoxy resin[21, 22], have become a hot research topic. Biomass is an important renewable resource left to us by nature. It has the inherent advantages of being renewable, low-cost and environmentally friendly,

and it is considered to be an effective substitute for non-renewable fossil resources. In order to prepare modified PF with both properties and low toxicity, it has undergone a process from partial or complete substitution of other petroleum phenols for the reaction of phenol with formaldehyde to partial or complete substitution of biomass phenol for the reaction of phenol with formaldehyde[20, 23]. Of course, the research on replacing formaldehyde is also an important research direction. Therefore, researchers have conducted a lot of research to find more economical and environmentally friendly renewable natural resources as raw material substitutes for phenol and formaldehyde in PF, including lignin[24, 25], cardanol[26], tannins[27, 28], bio-oil[29], furfural[20], p-benzene dialdehyde[12, 30, 31], 5-hydroxymethyl furfural[32, 33], glyoxal[34, 35], etc. But switching to more sustainable green raw materials while maintaining the desirable performance characteristics and reactivity of phenol and formaldehyde is a major challenge. The activity of biomass phenol is relatively lower than that of petroleum phenol. The activity of green-friendly aldehyde compounds is also incomparable with formaldehyde, and the low-toxic and harmless dialdehyde compound has only one aldehyde group to participate in the reaction in the synthesis stage[12, 30]. The product is an oligomer with a small molecular weight, which is mostly used as an adhesive[36–38], which simply cannot meet people's wide application requirements for green and high-performance PF. The preparation and application of bio-aldehyde-modified PF is greatly restricted, not to mention the green PF prepared from complete bio-phenols and bio-aldehydes. The reaction conditions can only be more severe[39]. Therefore, bio-phenol-modified PF is still one of the important directions of green high-performance modified PF.

Molecular structure and spatial network configuration have great influence on the properties of PF. Compared with traditional PF synthesized from phenol and formaldehyde, biomass PF have great advantages in the selectivity and diversification of molecular structure and spatial network configuration. Various functional PF can be prepared according to different application requirements, which is also one of the research directions of PF. Naringenin and daidzein are two kinds of natural compounds of flavonoid phenolic origin, and two benzene rings are interconnected by multiple carbon atoms, giving them high rigidity structural properties. Their molecular structures are shown in Fig. 1. Among the possible biomass alternatives, they are excellent renewable resources with more reaction sites. Naringenin is a flavonoid commonly found in citrus and grapefruit. Daidzein is a major isoflavone compound, a natural polyphenol monomer extracted from soybeans and other legumes. As biomass resources for replacing fossil resources, naringenin and daidzein have also been studied in the direction of bio-synthetic resins, and they have shown excellent performance. For example, it has been reported in some relevant literature that naringenin and daidzein can be used as bio-phenol raw materials for benzoxazine[40–43], the main synthetic components of epoxy resins[44–47], and flame retardants[48], showing excellent thermal properties, mechanical properties and flame retardant effects. It has not been reported that they are applied to PF.

In this work, in order to achieve the goal of sustainable development strategy, reduce environmental problems and health and safety hazards, we took advantage of the innate advantages of biomass non-toxic, sustainable and green to develop bio-based low-toxicity, functional PF resins. The natural

compounds of naringenin and daidzein from flavonoid were used to synthesize two bio-based PF under certain conditions, and the corresponding characterization methods were used to investigate their properties of curing behavior, thermogravimetric properties, chemical structure, mechanical properties and friction properties. Their practical application values were also evaluated.

2 Experimental Section

2.1 Materials

Phenol (99.0wt%), formaldehyde solution (37% wt% in H_2O), sodium hydroxide (NaOH, 96 wt%) and hydrochloric acid (HCl, 37% w/w) were purchased from Sinopharm Group Co., Ltd.. Daidzein (96wt%) and naringenin (97wt%) were obtained from China Aladdin Reagent. Distilled or deionized water was self-prepared. All the materials chemicals were used as received without any purification.

2.2 Synthesis of daidzein-based phenolic resin(D-PF)

Daidzein, formaldehyde solution, sodium hydroxide and deionized water were mixed well into a 250 mL three-necked flask equipped with a mechanical stirrer and a reflux condenser. The reaction was conducted at 105°C and kept for 1.5h in an oil bath. Then phenol was added to this three-necked flask. The temperature was raised to 115°C, and the reaction was stirred at this temperature for 2–3 hours. After the reaction, a certain amount of hydrochloric acid was added to neutralize sodium hydroxide. The product was dried at 60°C in a vacuum oven for 12 h. Finally, the D-PF rendered a gray-white powder after grinding. During the preparation process, the substitution ratio of daidzein to phenol gradually increased, so as to study the effect of daidzein on the modified phenolic resin. During the synthesis, it was ensured that the total molar ratio of phenols (phenol and daidzein) to formaldehyde was kept constant at 1:1.7. The molar ratio of daidzein and phenol was increased from 1:20 to 1:8, and they were named as D-PF-1-20, D-PF-1-18, D-PF-1-16, D-PF-1-14, D-PF-1-12, D-PF-1-10, D-PF-1-8.

2.3 Synthesis of naringenin-based phenolic resin(N-PF)

The N-PF was synthesized by the following procedure: a certain proportion (measured) of naringenin, formaldehyde solution and sodium hydroxide solution were mixed well and added into a 250 mL three-necked flask equipped with a mechanical stirrer and a reflux condenser. After heating to 80°C and keeping for 0.5 h in an oil bath, the phenol was added to this system. Then the temperature was raised to 120°C, and the reaction was stirred at this temperature for 1.5-3 hours. Finally, a yellow powder naringenin-based phenolic resin was obtained. Similarly, the substitution ratio of naringenin to phenol gradually increased. It was ensured that the total molar ratio of phenol (phenol and naringenin) to formaldehyde was kept constant at 1:1.7. The molar ratio of naringenin to phenol was increased from 1:20 to 1:8, and they were recorded as N-PF-1-20, N-PF-1-18, N-PF-1-16, N-PF-1-14, N-PF-1-12, N-PF-1-10 and N-PF-1-8. The synthesis process of D-PF and N-PF is shown in Fig. 2.

As a comparative reference for D-PF and N-PF performance testing, the conventional PF was also prepared. Phenol, formaldehyde (P : F = 1:1.7) and sodium hydroxide were mixed well and then added into three-necked flask. The mixture was stirred at 60°C for 0.5 h. Then the reaction mixture was warmed to 90°C, and the reaction time was 4 h.

2.4 Curing conditions of resins

The curing conditions were determined from the results of differential scanning calorimetry (DSC). The resin was ground to obtain a fine powder over 50 mesh, and the resin powder was evenly poured into the metal mold, and the initial curing was completed by hot pressing in a four-column hydraulic hot press at 140°C and 8MPa for 30 minutes. The resin was then transferred to a muffle furnace and cured at 170°C for 2h to obtain D-PF.

The curing conditions of the N-PF were similar to those of D-PF, and the initial curing was completed by hot pressing in a four-column hydraulic hot press at 140°C and 8MPa for 30 minutes. The resin was then transferred to a muffle furnace and cured at 160°C for 1h.

To prepare the conventional PF, the initial curing was completed by hot pressing in a four-column hydraulic hot press at 140°C and 8MPa for 30 minutes. The resin was then transferred to a muffle furnace and cured at 140°C. The curing time of sample for PF-1in muffle furnace is 1 hour, while the curing time of sample for PF-2 in muffle furnace is 2 hours.

2.5 Characterization

The different functional groups were examined via a Fourier transform infrared (FT-IR) spectrophotometer (Nicolet AVATAR360, Madison) to confirm the chemical structure of the D-PF and N-PF. The FT-IR spectra of samples were obtained via the economical KBr tableting method in the wavenumber range of 400–4000 cm^{-1}.

Curing behavior and thermogravimetric analysis of the D-PF and N-PF were conducted via thermogravimetry–differential scanning calorimetry (TG-DSC) thermal analyzer (STA, 449 F3) with heating rate of 10℃/min under N_2 atmosphere. Differential scanning calorimetry (DSC) and thermogravimetric analysis (TGA) were conducted in the temperature ranges of 25–300℃ and 25–800℃, respectively.

The mechanical properties were evaluated via using a universal testing machine (AGS-X, SHIMADZU). Tensile strength and flexural strength were important performance indicators to evaluate thermosetting resins. Each specimen was made in the size of 80mm×10mm×4mm. To ensure the accuracy of the measured values, at least 5 measurements were performed on each sample. The tensile rate was 1mm/min, and the movement rate of three-point bending was also 1mm/min. A rock-well hardness tester was used to test the rock-well hardness.

Tensile fracture surface morphology and flexural fracture surface morphology were characterized via using a scanning electron microscopy (SEM, NovaNano450/FEI).

Average friction coefficient and dynamic friction coefficient of modified phenolic resin were tested via friction and wear tester (MS-T3001, Lanzhou Huahui Instrument Technology, China). Tests were carried out at sliding velocity of 200r/min and uniform load of 500g. Width and depth of the worn surface of the D-PF and N-PF were examined via using an optical microscope (Zeiss observer Z1m) and 3D profilometer (Keyence VHX-1000) to calculate the wear rate of their surface.

3 Results And Discussion

3.1 Infrared spectroscopy analysis

D-PF and N-PF have similar molecular structures, and their infrared spectra show roughly the same characteristic peaks. The FTIR spectra of the cured D-PF, N-PF and PF are shown in Fig. 3

The characteristic peak of D-PF at 1631 cm^{-1} and the peak of N-PF at 1630 cm^{-1} correspond to C = C-C = O group and C = O group[40, 42, 44, 46], respectively. We can find these two characteristic peaks at the same position in the infrared spectra of daidzein and naringenin (Fig. 3a). The two peaks at 1608 cm^{-1} and 1477 cm^{-1} are ascribed to C = C stretching vibration of the benzene ring backbone of D-PF, N-PF and PF. The characteristic peaks around 3422 cm^{-1} belongs to -OH group. The absorption band at 1210 cm^{-1} is the vibrational peak of C-O-C in the pyran ring and C-O of the phenolic hydroxyl group on the phenol ring. The characteristic peaks of $-CH_2$ appears around 2922 cm^{-1}. The absorption peaks in the low band (600-900cm^{-1}) are generally considered to be related to the substitution of hydrogen atoms on the phenol ring. The two peaks at 824 and 755 cm^{-1} belong to the characteristic peaks of para and ortho C–H substitutions on the phenolic rings. According to above analyses, the synthesized modified resin successfully introduced the rigid structure of flavonoid phenols (daidzein and naringenin).

3.2 Curing Behaviors

The curing behaviors of D-PF, N-PF and PF were monitored by DSC, and their corresponding DSC exotherms were recorded for analysis. As shown in Fig. 4, the DSC curves of D-PF, N-PF and PF all show the results of a single exothermic peak. The DSC curves of the two flavonoid phenol modified resins D-PF and N-PF have some similar rules. The curing initiation temperature T_i of D-PF, and N-PF is about 120 to 130°C. The curing termination temperature T_e is about 190°C to 200°C, while the T_i of PF is 110°C with the curing peak temperature T_p of 139.5 and T_e of 160°C. Compared with the low curing peak temperature of ordinary PF, the curing temperature of D-PF, N-PF are greatly increased. Interestingly, the curing peaks of D-PF and N-PF show opposite results. As shown in Fig. 4c and 4d, with the increasing of the proportion of daidzein in the reaction, the curing peak temperature of D-PF shows an overall downward trend, while the curing peak temperature of N-PF shows a trend of overall improvement with

the increasing of substitution rate of naringenin. The modified resin exhibits higher T_i, T_p and T_e than those of PF.

It is well known that under the same conditions, the peak temperature monitored by DSC can be used to judge the strength of the curing reactivity of phenolic resin. This means that the lower the peak temperature is, the higher the reactivity is. Therefore, the reactivity of the raw material of the synthetic resin is the main reason for this result. Biomass phenols are generally less active than petroleum phenols. Therefore, higher energy and conditions are required during synthesis and curing. Secondly, the reaction site and steric hindrance are also important reasons. The bio-phenols of daidzein and naringenin have large rigid skeletal structures, and the steric hindrance generated by the rigid group slows down the curing reaction to a certain extent, which is the reason why their curing temperature is higher than PF. The difference in reaction sites and steric hindrance and reactivity may be the reason why the curing peak temperatures T_p of D-PF and N-PF proceeds in opposite directions. The reaction activity of naringenin is higher than that of daidzein. With a small amount of naringenin added, the curing peak temperature of N-PF is lower. With the increasing of the addition ratio, the steric hindrance effect caused by the large volume of naringenin makes the polycondensation more difficult, and the curing peak temperature of N-PF is increased accordingly. The activity of daidzein is low, the energy required for curing reaction is high, resulting in the high curing peak temperature. However, with the increasing of the proportion of daidzein, the opportunity for daidzein to participate in the polycondensation reaction is increased, and the curing peak temperature of D-PF is gradually decreased.

3.3 Thermal Stability of the Cured Resins

Thermal performance is an important indicator of thermosetting resins and an important means to evaluate the thermal stability of phenolic resins. Thermogravimetric analysis (TGA) was performed to evaluate the thermal stability of the successfully modified phenolic resins. The TGA and DTG curves of cured N-PF, D-PF and PF are shown in Fig. 5. The thermal degradation characteristic parameters of cured N-PF, D-PF and PF include $T_{5\%}$ (temperature at which 5% weight loss occurs), $T_{10\%}$ (temperature at which 10% weight loss occurs), $T_{d,max}$ (temperature of maximum degradation rate) and Y_{C800} (residue at 800°C) are recorded in the Table 1 to provide the relevant thermal stability performance analysis.

As shown in Fig. 5, N-PF and D-PF with different ratios have similar TGA and DTG curves, which indicates that they have similar thermal decomposition laws. For N-PF and D-PF, the thermal decomposition at low temperature ($T_{5\%}$ and $T_{10\%}$) shows a trend of increasing firstly and then decreasing (the detailed temperature values are described in Table 1). The $T_{5\%}$ and $T_{10\%}$ values of N-PF and D-PF are higher than those of PF-1 and PF-2, indicating that their thermal properties at low temperature are much better than those of PF-1 and PF-2. There is a small gap between the Y_{C800} values of different ratios of N-PF. The carbon yield Y_{C800} for N-PF is approximately 59%, which is slightly higher than that of PF-1 (56%). D-PF resin has a high residual carbon at 800°C, and the highest Y_{C800} is 64.39%, which is higher than that of PF-2 with 58.15%.

Table 1
Thermal stability related data of resins

Resin	$T_{5\%}$(℃)	$T_{10\%}$(℃)	$T_{d,max}$(℃)	Char Residues at 800℃(wt%)
PF-1	136.76	219.24	513.59	56.85
PF-2	127.36	212.66	508.59	58.15
N-PF-1-20	154.00	250.64	520.59	58.89
N-PF-1-18	149.91	251.64	522.59	58.24
N-PF-1-16	168.31	251.61	523.41	57.81
N-PF-1-14	204.77	297.61	511.29	59.81
N-PF-1-12	203.95	284.53	519.79	59.56
N-PF-1-10	200.64	279.72	515.90	59.48
N-PF-1-8	195.04	269.66	510.00	58.18
D-PF-1-20	187.53	332.94	519.23	61.75
D-PF-1-18	223.54	365.51	524.94	62.14
D-PF-1-16	226.42	337.93	520.71	61.03
D-PF-1-14	202.31	350.43	533.48	61.92
D-PF-1-12	160.90	312.32	543.09	62.95
D-PF-1-10	154.52	297.82	540.50	64.39
D-PF-1-8	152.69	269.15	535.02	59.94

The weight loss caused by the thermal decomposition of N-PF, D-PF and PF in the low temperature section (below 300°C) is the volatilization and release of formaldehyde and water in the resin, as well as the possible existence of small molecules released from the condensation reaction. Compared with phenol, the bio-phenols daidzein and naringenin have large and complex structures, and their rigid groups have better heat resistance. It is well known that the higher the degree of crosslinking is, the better the heat resistance is. It can be seen that the appropriate introduction of daidzein and naringenin can improve the degree of crosslinking and improve heat resistance. However, with the increasing of the proportion of daidzein and naringenin, the huge rigid structure can produce inhomogeneous products during the synthesis and curing stages, resulting in the increasing of voids in the three-dimensional space network of the synthetic resin. Therefore, in the thermal decomposition in the middle and low temperature range, the $T_{5\%}$ and $T_{10\%}$ of N-PF and D-PF are firstly increased and then decreased. The decomposition of the N-PF and D-PF resin at high temperature (400℃-600℃) is mainly due to the degradation of cross-linking, the cleavage and decomposition of ether bonds and methylene groups, which is the reason for the maximum decomposition rate. As shown in the Fig. 5b, d and Table 1, the N-PF, D-PF and PF all have

a large decomposition peak at 400°C to 600°C. The $T_{d,max}$ of N-PF is approximately 523℃, while the corresponding $T_{d,max}$ of PF-1 is 513.59℃. The $T_{d,max}$ of D-PF is approximately 543℃, while the $T_{d,max}$ of PF-2 is only 508.59℃. This is attributed to the pyrone ring structure connecting two benzene rings in the structures of daidzein and naringenin, which ensures their higher rigidity and heat resistance. In the final temperature range of 600–800°C, the decomposition weight loss curve tends to be flat, indicating that the proportion of weight loss is small, which is due to the residual resin is pyrolyzed to form an amorphous residual carbon. Overall, the heat resistance of the modified phenolic resin prepared from the rigid structure of daidzein or naringenin is excellent.

3.4 Mechanical Properties

Mechanical properties are one of the most important performance indicators of phenolic resins, and the strength of mechanical properties directly restricts the application fields of phenolic resins. Therefore, in order to avoid the influence of errors, tensile and flexural tests are used to jointly evaluate the mechanical properties of the modified resin. The comparison of tensile and flexural properties between N-PF, D-PF and PF after curing are shown in Fig. 6 and Table 2. The tensile strength and flexural strength of N-PF and D-PF resins are increased firstly and then decreased with the increasing of the proportion of daidzein and naringenin. The maximum tensile and flexural strengths of N-PF are 33.86 MPa and 110.42 MPa, respectively, compared with PF-1 (28.77 and 79.89 MPa). Similarly, the maximum tensile and flexural strengths of D-PF are 35.61 and 103.17 MPa, respectively, while the strengths for PF-2 are 24.48 and 55.79 MPa. However, we found that with the increasing of proportion of daidzein and naringenin, the tensile and flexural strengths of N-PF and D-PF resins are lower than those of unmodified common PF resins. This shows that in the process of modifying PF resin, the substitution rate of phenol is not as high as possible. The strength of the modified resin is lower than that of the unmodified resin due to the excessive proportion of daidzein and naringenin in the reaction system. We have mentioned this insight in the thermal analysis section. The bulky rigid structure can cause steric hindrance and product inhomogeneity during the synthesis and curing stages, resulting in the increased voids in the three-dimensional spatial network of the synthetic resin. This means that the synthetic modified resin has some defects, which is the reason why the strength of the modified resin is lower than that of the unmodified resin. Rockwell hardness results are also recorded in the Table 2. The Rockwell hardness of N-PF and D-PF resins with bio-based rigid structure is not much different from that of ordinary PF resins. The hardness of the modified resin is moderate, which avoids the problem of excessive noise in some applications.

Table 2
Mechanical properties of resins

Resin	Tensile strength/MPa	Flexural strength/MPa	Rockwell hardness/HRR
PF-1	25.86–32.14	77.45–83.06	121.02
PF-2	21.24–29.57	51.19–61.18	122.78
N-PF-1-20	18.18–26.32	93.03-101.38	119.9
N-PF-1-18	31.59–35.93	102.30-117.34	121.9
N-PF-1-16	30.17–34.51	100.37-111.05	122.62
N-PF-1-14	31.35–35.62	93.26-108.83	120.4
N-PF-1-12	29.08–34.39	84.57–87.89	119.23
N-PF-1-10	22.35–27.85	75.02–84.97	121.26
N-PF-1-8	18.11–21.46	63.38–73.39	119.0
D-PF-1-20	17.51–19.23	88.57–89.08	121.74
D-PF-1-18	18.71–21.03	101.74-107.31	119.0
D-PF-1-16	33.46–38.86	88.41–97.75	119.78
D-PF-1-14	31.09–33.65	88.03–99.94	120.38
D-PF-1-12	33.72–35.76	79.05–90.47	119.88
D-PF-1-10	19.29–23.05	51.87–68.19	119.34
D-PF-1-8	20.56–21.16	58.78–70.94	118.98

3.5 SEM Analysis of Resins surface section morphology

(a) N-PF(b)D-PF(c)PF of tensile fracture morphology;(d) N-PF(e)D-PF(f)PF of flexural fracture morphology

SEM images of tensile and flexural fracture surface morphology are used to explain the differences in the mechanical properties of the analytical resins at the microscopic level. The SEM images of tensile fracture sections and flexural fracture sections of N-PF, D-PF and PF resins are shown in Fig. 7. The tensile and flexural sections of PF are smooth, and the crack propagation direction is in a single direction, showing a brittle fracture state. After introducing the rigid structure of daidzein and naringenin, the roughness of tensile fracture section and flexural fracture section of D-PF and N-PF increase significantly. The fracture direction tends to disperse. The rougher fracture surface with dislocations and vacancies indicates that the modified resins N-PF, D-PF have higher toughness, and their corresponding tensile and flexural strengths are also improved. This verifies the analysis results in the mechanical properties analysis section. At the same time, the three-dimensional spatial defects mentioned in thermal analysis and mechanical analysis are confirmed by SEM. In the tensile and flexural fracture section of N-PF, D-PF,

we can see some void defects, which is the reason for the decline of the mechanical properties of the resin.

3.6 Tribological properties

In this test, D-PF-1-20 and N-PF-1-20 are selected as modified resins for performance comparison with ordinary PF resins. The dynamic coefficient of friction and the average coefficient friction of resins are recorded in Fig. 8 and Table 3.

Table 3
Tribological properties related data of resins

Resin	Average coefficient of friction	Wear rate(mm^3/ Nm)
N-PF-1-20	0.1511	$9.428*10^{-6}$
PF-1	0.1550	$1.862*10^{-5}$
D-PF-1-20	0.1211	$1.113*10^{-5}$
PF-2	0.1528	$1.068*10^{-5}$

From the Fig. 8, we can find that the dynamic friction coefficients of the four resins are very stable in the friction test for up to 0.5h, and fluctuates steadily within a certain range. From the test results of friction properties of these four resins, the dynamic friction coefficient of D-PF-1-20 fluctuates the least with time, indicating that its contact surface is smoother and its friction coefficient is also the smallest. The dynamic friction coefficient of N-PF-1-20 fluctuates widely in the early stage of the test, but it is stable in the later stage. The cause may be uneven contact surface roughness and deep scratches caused by voids inside the resin. The dynamic friction coefficient of ordinary PF resin tends to be normal with time. The average friction coefficients of D-PF-1-20, N-PF-1-20, PF-1 and PF-2 are 0.1211, 0.1511, 0.1550, 0.1528, respectively. Obviously, with the addition of bio-based daidzein and naringenin, the friction coefficient of the resin is decreased, and it is more stable than that of the common PF resin with the same curing process. The sound produced during the friction test is moderate and not sharp. The moderate hardness prevents the resin from making annoying, disgusting noises during using.

The tribological properties of modified resins are reflected by the friction coefficient and wear rate. The width and depth of the worn surface of the four resins (D-PF-1-20, N-PF-1-20, PF-1 and PF-2) were obtained by optical microscope and 3D profilometer to calculate the wear rate. The wear rate is calculated according to the following equation:

$$V = 2\pi Rbh$$

and

$$K = V/(Ld)$$

Where V is the wear volume (mm^3), R is the wear scar radius of the worn surface (mm), b is the wear scar width of the worn surface (mm), h is the depth of the wear scar on the worn surface, and K is the wear rate (mm^3/ Nm), L is the load applied to the resin (N), and d is the sliding distance (m).

The wear rates of D-PF-1-20, N-PF-1-20, PF-1 and PF-2 are recorded in Table 3. It can be concluded that the wear rate of N-PF-1-20 resin is lower than that of PF-1, while the wear rate of D-PF-1-20 is comparable to that of PF-2. The wear rates of D-PF-1-20, N-PF-1-20, PF-1 and PF-2 are $1.113*10^{-5}$, $9.42*10^{-6}$, $1.862*10^{-5}$, $1.068*10^{-5}mm^3$/ Nm, respectively. Although D-PF-1-20 resin has the smallest coefficient of friction, its wear rate is slightly higher than that of PF-2 resin. The N-PF-1-20 resin with a friction coefficient similar to that of PF-1 resin has an excellent wear rate. From the 3D profile, we can observe the changes in the depth and width of the wear scar of the four resins. The normal PF resins with two different curing conditions represents the deepest wear marks and the widest wear mark widths, respectively, while the two modified resins show moderate wear marks depth and wear mark widths. This indicates that the addition of daidzein and naringenin can appropriately reduce the wear marks depth and wear marks width of PF resin. We can also observe the overall condition of the surface of the resin wear part from the Fig. 9. The plough marks on the wear surface of the PF resin are more obvious, and the wear track is rougher and larger. Compared with pure PF resin, the surface of the worn part of D-PF-1-20 and N-PF-1-20 is smoother and more uniform. This is mainly attributed to the rigid structure and excellent three-dimensional network structure of the modified resin which hinders the movement of molecular chains, ensuring its excellent wear and friction properties. At the same time, the purpose of testing the friction properties of the modified resin is to consider the application of the modified resin in tribology and brake materials. Friction materials, brake materials can easily reach a higher temperature of 300 ℃ during using. In the analysis of thermal properties, we have proved that the modified resins D-PF and N-PF have excellent heat resistance in the middle temperature. The result shows that the D-PF and N-PF resins modified and enhanced by daidzein and naringenin have lower friction coefficient and more excellent wear resistance than pure PF. In the preparation of friction braking materials, the two modified resins can be used as polymer matrix with excellent properties.

4 Conclusions

In this work, in order to save the use of fossil resources and reduce the amount of phenol used in the preparation of phenolic resins, we developed two green and economical phenolic resins to broaden the research field and application scope of PF resins. The prepared bio-based phenolic resins were characterized by DSC, TG, SEM, mechanical performance and tribological performance and evaluated for the potential applications. The introduction of rigid backbone groups during the synthesis of N-PF and D-PF can delay their curing reaction and results in higher curing peak temperatures. The results of TG test ($T_{5\%}$, $T_{10\%}$, $T_{d,max}$ and Y_{C800}) show that compared with common PF, N-PF and D-PF have higher thermal decomposition temperature and residual rate, as well as better thermal stability. The high degradation temperature and high carbon yield of N-PF and D-PF allow them to be used in many high temperature resistant fields, such as aerospace composite materials and ablative materials. The proportions of

daidzein and naringenin have great effects on the mechanical properties of N-PF and D-PF. The maximum tensile strength and flexural strengths of D-PF are 35.61 MPa and 103.17 MPa respectively, while the maximum tensile strength and flexural strengths of N-PF are 33.86 MPa and 110.42 MPa respectively. In the friction performance test, the lower friction coefficient and wear rate indicate that they have excellent tribological properties and can be used as brake materials and excellent polymer matrix for friction materials. In conclusion, the prepared N-PF and D-PF have excellent processability, tribological properties, mechanical properties and ablative properties, and are suitable for high-performance ablative composites and resin matrices for friction composites.

Declarations

Acknowledgment

The work was supported by National Natural Science Foundation of China(No. 20207003, No. 20704019, No. 51603093), Innovative and Entrepreneurial Building Team Project of Jiangsu Province(No. 2015026) and New Green Materials Project of Hangmo New Materials Group Co., Ltd.. The authors wish to express their appreciation to the Analytical Center at Jiangsu University for the measurements of samples.

References

1. B. Kiskan, Y. Yagci, The journey of phenolics from the first spark to advanced materials. Isr. J. Chem. **60**(1–2), 20–32 (2020)
2. Y. He, R. Duan, Q. Zhang, T. Xia, B. Yan, S. Zhou, J. Huang, Reinforce the mechanical toughness, heat resistance, and friction and wear resistance of phenolic resin via constructing self-assembled hybrid particles of graphite oxide and zirconia as nano-fillers. Adv. Compos. Hybrid. Ma **4**(2), 317–323 (2021)
3. L.P. de Hoyos-Martínez, H. Issaoui, R. Herrera, J. Labidi, F. Charrier-El, Bouhtoury, Wood fireproofing coatings based on biobased phenolic resins. ACS Sustain. Chem. Eng. **9**(4), 1729–1740 (2021)
4. A. Beda, P.L. Taberna, P. Simon, C. Matei Ghimbeu, Hard carbons derived from green phenolic resins for Na-ion batteries. Carbon. **139**, 248–257 (2018)
5. Z. Wei, H.X. Zhao, Y.B. Niu, S.Y. Zhang, Y.B. Wu, H.J. Yan, S. Xin, Y.X. Yin, Y.G. Guo, Insights into the pre-oxidation process of phenolic resin-based hard carbon for sodium storage. Mater. Chem. Front. **5**(10), 3911–3917 (2021)
6. Y. Xu, L. Guo, H. Zhang, H. Zhai, H. Ren, Research status, industrial application demand and prospects of phenolic resin. RSC Adv. **9**(50), 28924–28935 (2019)
7. F.F. Binda, V.D.A. Oliveira, C.A. Fortulan, L.B. Palhares, C.G. dos Santos, Friction elements based on phenolic resin and slate powder. J. Mater. Res. Technol. **9**(3), 3378–3383 (2020)
8. W.M. Moreira, P.V. Viotti, A.A. de Moura, M.L. Gimenes, M.G.A. Vieira, Synthesis of a biobased resin and its screening as an alternative adsorbent for organic and inorganic micropollutant removal.

Environ. Sci. Pollut Res. Int. **29**, 79935–79953 (2022)

9. D. Torres, S. Pérez-Rodríguez, L. Cesari, C. Castel, E. Favre, V. Fierro, A. Celzard, Review on the preparation of carbon membranes derived from phenolic resins for gas separation: From petrochemical precursors to bioresources. Carbon. **183**, 12–33 (2021)
10. L. Guo, Y. Yang, F. Xu, Q. Lan, M. Wei, Y. Wang, Design of gradient nanopores in phenolics for ultrafast water permeation. Chem. Sci. **10**(7), 2093–2100 (2019)
11. X. Xing, Y. Zhao, X. Zhang, J. Wang, T. Hong, Y. Li, S. Wang, C. Zhang, X. Jing, Healable ablative composites from synergistically crosslinked phenolic resin. Chem. Eng. J. **447**, 137571 (2022)
12. L. Granado, R. Tavernier, S. Henry, R.O. Auke, G. Foyer, G. David, S. Caillol, Toward Sustainable Phenolic Thermosets with High Thermal Performances. ACS Sustain. Chem. Eng. **7**(7), 7209–7217 (2019)
13. C. Nair, Advances in addition-cure phenolic resins. Prog Polym. Sci. **29**(5), 401–498 (2004)
14. J. Chen, K. Zhang, K. Zhang, B. Jiang, Y. Huang, Facile preparation of reprocessable and degradable phenolic resin based on dynamic acetal motifs. Polym. Degrad. Stabil **196**, 109818 (2022)
15. K. Błażek, J. Datta, Renewable natural resources as green alternative substrates to obtain bio-based non-isocyanate polyurethanes-review. Crit. Rev. Environ. Sci. Technol. **49**(3), 173–211 (2019)
16. A. Noreen, K.M. Zia, M. Zuber, S. Tabasum, A.F. Zahoor, Bio-based polyurethane: An efficient and environment friendly coating systems: A review. Prog Org. Coat. **91**, 25–32 (2016)
17. C. Zhang, J. Xue, X. Yang, Y. Ke, R. Ou, Y. Wang, S.A. Madbouly, Q. Wang, From plant phenols to novel bio-based polymers. Prog Polym. Sci. **125**, 101473 (2022)
18. M. Derradji, O. Mehelli, W. Liu, N. Fantuzzi, Sustainable and ecofriendly chemical design of high performance bio-based thermosets for advanced applications. Front. Chem. **9**, 691117 (2021)
19. J. Liu, S. Wang, Y. Peng, J. Zhu, W. Zhao, X. Liu, Advances in sustainable thermosetting resins: From renewable feedstock to high performance and recyclability. Prog Polym. Sci. **113**, 101353 (2021)
20. P.R. Sarika, P. Nancarrow, A. Khansaheb, T. Ibrahim, Bio-based alternatives to phenol and formaldehyde for the production of resins. Polym. -Basel **12**(10), 2237 (2020)
21. F.A.M.M. Gonçalves, M. Santos, T. Cernadas, P. Ferreira, P. Alves, Advances in the development of biobased epoxy resins: insight into more sustainable materials and future applications. Int. Mater. Rev. **67**(2), 119–149 (2021)
22. G. Mashouf Roudsari, A.K. Mohanty, M. Misra, Green approaches to engineer tough biobased epoxies: a review. ACS Sustain. Chem. Eng. **5**(11), 9528–9541 (2017)
23. K. Tang, A. Zhang, T. Ge, X. Liu, X. Tang, Y. Li, Research progress on modification of phenolic resin. Mater. Today Commun. **26**, 101879 (2021)
24. G. Foyer, B.H. Chanfi, D. Virieux, G. David, S. Caillol, Aromatic dialdehyde precursors from lignin derivatives for the synthesis of formaldehyde-free and high char yield phenolic resins. Eur. Polym. J. **77**, 65–74 (2016)

25. W. Yang, L. Jiao, X. Wang, W. Wu, H. Lian, H. Dai, Formaldehyde-free self-polymerization of lignin-derived monomers for synthesis of renewable phenolic resin. Int. J. Biol. Macromol. **166**, 1312–1319 (2021)
26. C. Bo, L. Hu, Y. Chen, X. Yang, M. Zhang, Y. Zhou, Synthesis of a novel cardanol-based compound and environmentally sustainable production of phenolic foam. J. Mater. Sci. **53**(15), 10784–10797 (2018)
27. V. Barbosa, E.C. Ramires, I.A.T. Razera, E. Frollini, Biobased composites from tannin–phenolic polymers reinforced with coir fibers. Ind. Crop Prod. **32**(3), 305–312 (2010)
28. E.C. Ramires, E. Frollini, Tannin–phenolic resins: Synthesis, characterization, and application as matrix in biobased composites reinforced with sisal fibers. Compos. Part. B-Eng **43**(7), 2851–2860 (2012)
29. J. Xu, N. Brodu, M. Mignot, B. Youssef, B. Taouk, Synthesis and characterization of phenolic resins based on pyrolysis bio-oil separated by fractional condensation and water extraction. Biomass Bioenergy. **159**, 106393 (2022)
30. L. Granado, R. Tavernier, G. Foyer, G. David, S. Caillol, Catalysis for highly thermostable phenol-terephthalaldehyde polymer networks. Chem. Eng. J. **379**, 122237 (2020)
31. R. Oye Auke, G. Arrachart, R. Tavernier, G. David, S. Pellet-Rostaing, Terephthalaldehyde-phenolic resins as a solid-phase extraction system for the recovery of rare-earth elements. Polymers-Basel. **14**(2), 311 (2022)
32. Y. Zhang, Z. Yuan, N. Mahmood, S. Huang, C. Xu, Sustainable bio-phenol-hydroxymethylfurfural resins using phenolated de-polymerized hydrolysis lignin and their application in bio-composites. Ind. Crop Prod. **79**, 84–90 (2016)
33. Z. Yuan, Y. Zhang, C. Xu, Synthesis and thermomechanical property study of Novolac phenol-hydroxymethyl furfural (PHMF) resin. RSC Adv. **4**(60), 31829–31835 (2014)
34. M. Siahkamari, S. Emmanuel, D.B. Hodge, M. Nejad, Lignin-glyoxal: a fully biobased formaldehyde-free wood adhesive for interior engineered wood products. ACS Sustain. Chem. Eng. **10**(11), 3430–3441 (2022)
35. I. Van Nieuwenhove, T. Renders, J. Lauwaert, T. De Roo, J. De Clercq, A. Verberckmoes, Biobased resins using lignin and glyoxal. ACS Sustain. Chem. Eng. **8**(51), 18789–18809 (2020)
36. H. Zhang, P. Liu, S.M. Musa, C. Mai, K. Zhang, Dialdehyde cellulose as a bio-based robust adhesive for wood bonding. ACS Sustain. Chem. Eng. **7**(12), 10452–10459 (2019)
37. P. Li, Y. Wu, Y. Zhou, Y. Zuo, Preparation and characterization of resorcinol-dialdehyde starch-formaldehyde copolycondensation resin adhesive. Int. J. Biol. Macromol. **127**, 12–17 (2019)
38. N.A. Aziz, A.F.A. Latip, L.C. Peng, N.H. A.Latif, N. Brosse, R. Hashim, M.H. Hussin, Reinforced lignin-phenol-glyoxal (LPG) wood adhesives from coconut husk. Int. J. Biol. Macromol. **141**, 185–196 (2019)
39. A.N. Wilson, M.J. Price, C. Mukarakate, R. Katahira, M.B. Griffin, J.R. Dorgan, J. Olstad, K.A. Magrini, M.R. Nimlos, Integrated biorefining: coproduction of renewable resol biopolymer for aqueous stream

valorization. ACS Sustain. Chem. Eng. **5**(8), 6615–6625 (2017)

40. J. Dai, N. Teng, Y. Peng, Y. Liu, L. Cao, J. Zhu, X. Liu, Biobased benzoxazine derived from daidzein and furfurylamine: microwave-assisted synthesis and thermal properties investigation. Chem. Sus Chem. **11**(18), 3175–3183 (2018)
41. M. Han, S. You, Y. Wang, K. Zhang, S. Yang, Synthesis of highly thermally stable daidzein-based main-chain-type benzoxazine resins. Polymers-Basel. **11**(8), 1341 (2019)
42. K. Zhang, Y. Liu, M. Han, P. Froimowicz, Smart and sustainable design of latent catalyst-containing benzoxazine-bio-resins and application studies. Green. Chem. **22**(4), 1209–1219 (2020)
43. B. Hao, R. Yang, K. Zhang, A naringenin-based benzoxazine with an intramolecular hydrogen bond as both a thermal latent polymerization additive and property modifier for epoxy resins. RSC Adv. **10**(43), 25629–25638 (2020)
44. Y. Du, G. Zhao, G. Shi, Y. Wang, W. Li, S. Ren, Effect of crosslink structure on mechanical properties, thermal stability and flame retardancy of natural flavonoid based epoxy resins. Eur. Polym. J. **162**, 110898 (2022)
45. Y. Oh, K.M. Lee, D. Jung, J.A. Chae, H.J. Kim, M. Chang, J.J. Park, H. Kim, Sustainable, naringenin-based thermosets show reversible macroscopic shape changes and enable modular recycling. ACS Macro Lett. **8**(3), 239–244 (2019)
46. J. Dai, Y. Peng, N. Teng, Y. Liu, C. Liu, X. Shen, S. Mahmud, J. Zhu, X. Liu, High-performing and fire-resistant biobased epoxy resin from renewable sources. ACS Sustain. Chem. Eng. **6**(6), 7589–7599 (2018)
47. C. Xu, Y. Xu, M. Chen, Y. Zhang, J. Li, Q. Gao, S.Q. Shi, Soy protein adhesive with bio-based epoxidized daidzein for high strength and mildew resistance. Chem. Eng. J. **390**, 124622 (2020)
48. C. Ma, J. Li, Synthesis of an organophosphorus flame retardant derived from daidzein and its application in epoxy resin. Compos. Part. B-Eng **178**, 107471 (2019)

Figures

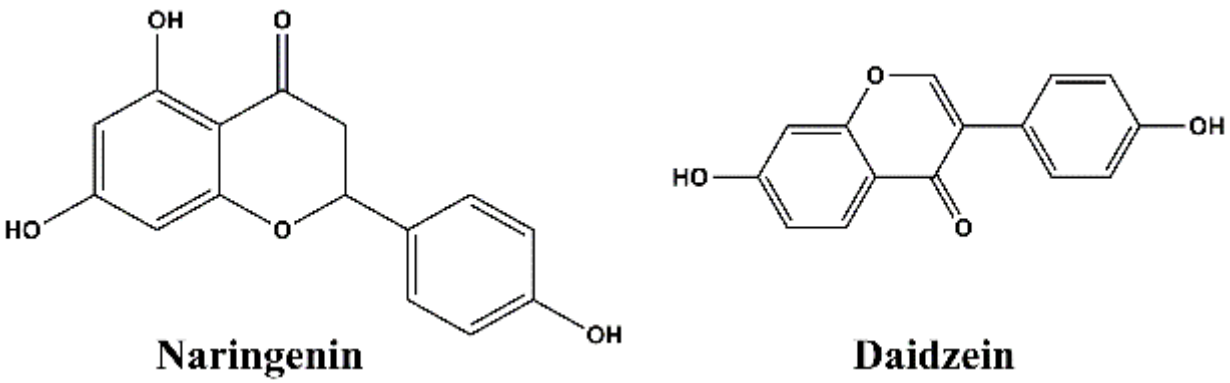

Figure 1

Chemical structures of daidzein and naringenin

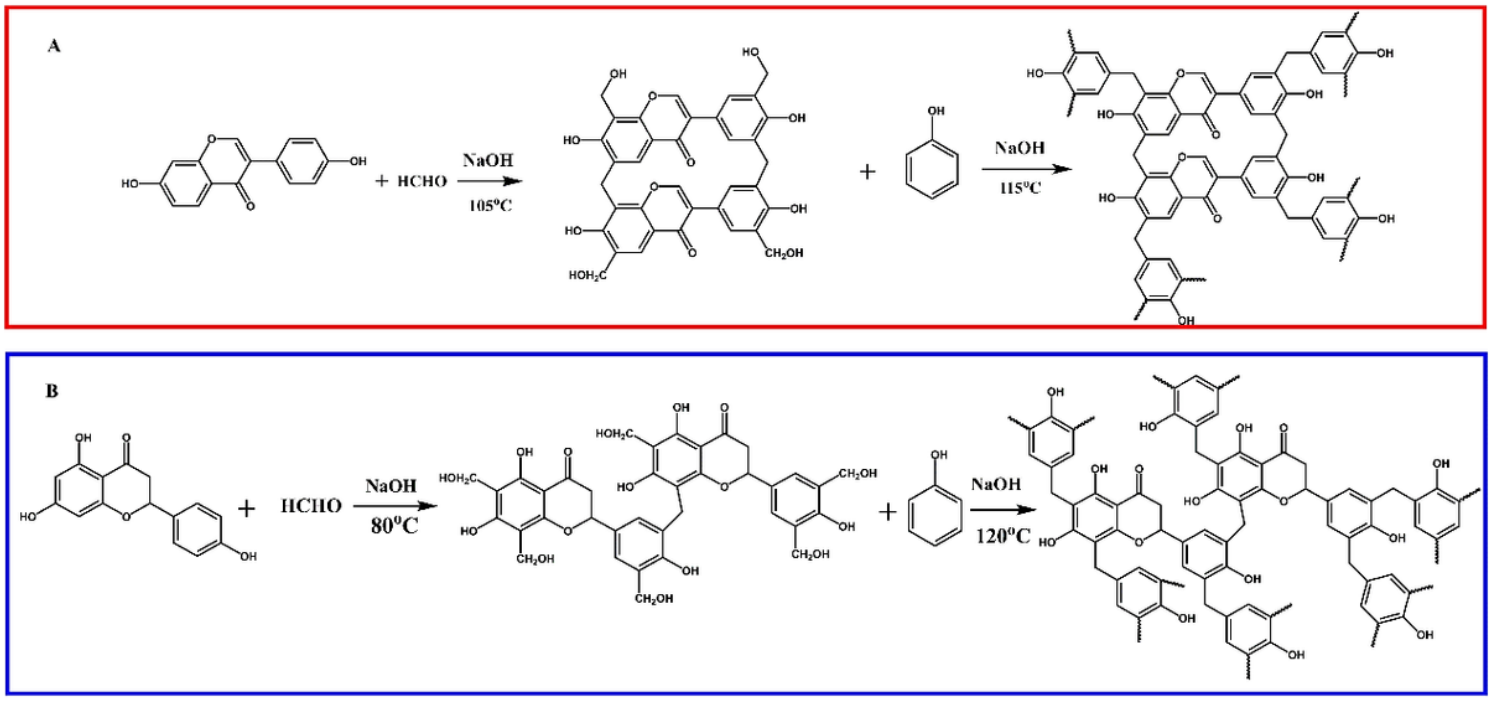

Figure 2

Synthesis of D-PF and N-PF

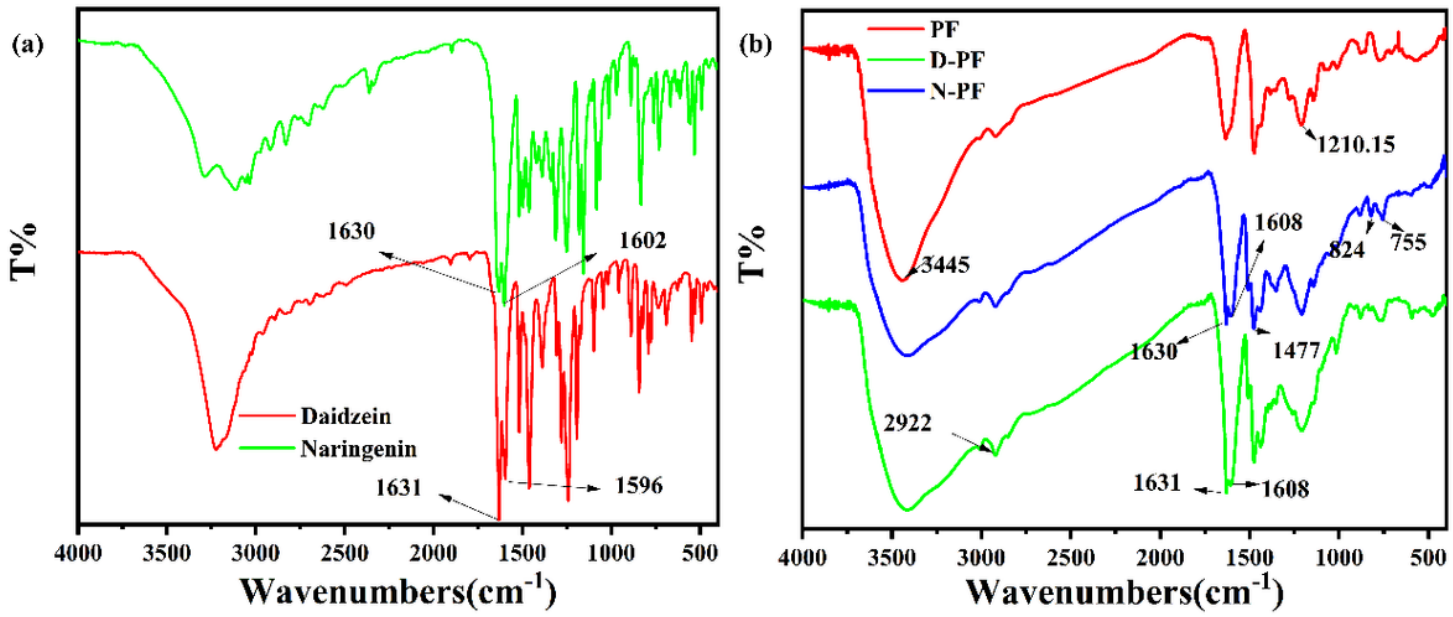

Figure 3

(a) FT-IR spectra of daidzein and naringenin. (b) FT-IR spectra of PF, D-PF and N-PF

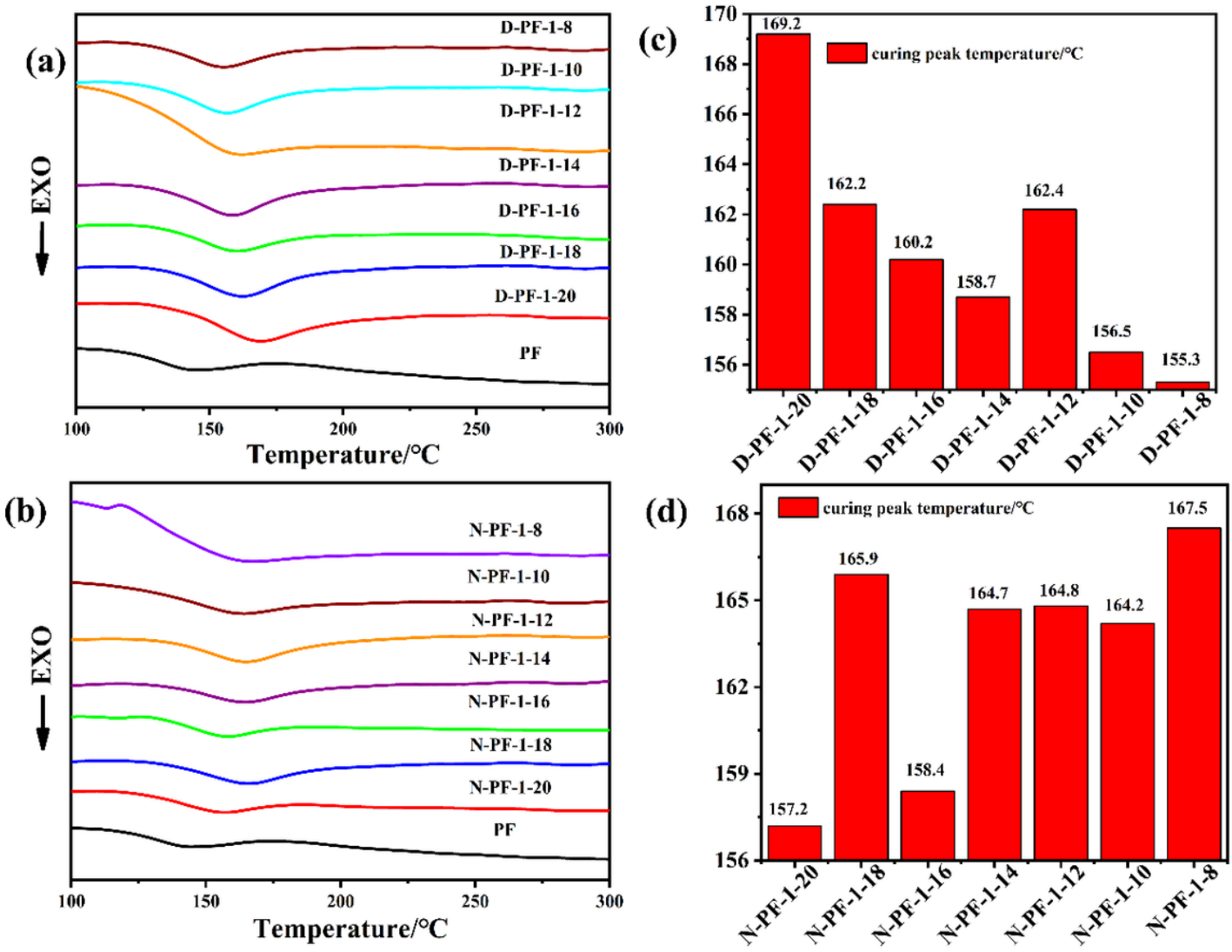

Figure 4

Differential scanning calorimetry (DSC) thermograms of D-PF(a) and N-PF (b)with different proportions. (b) Curing peaks of D-PF(c) and N-PF (d)with different proportions

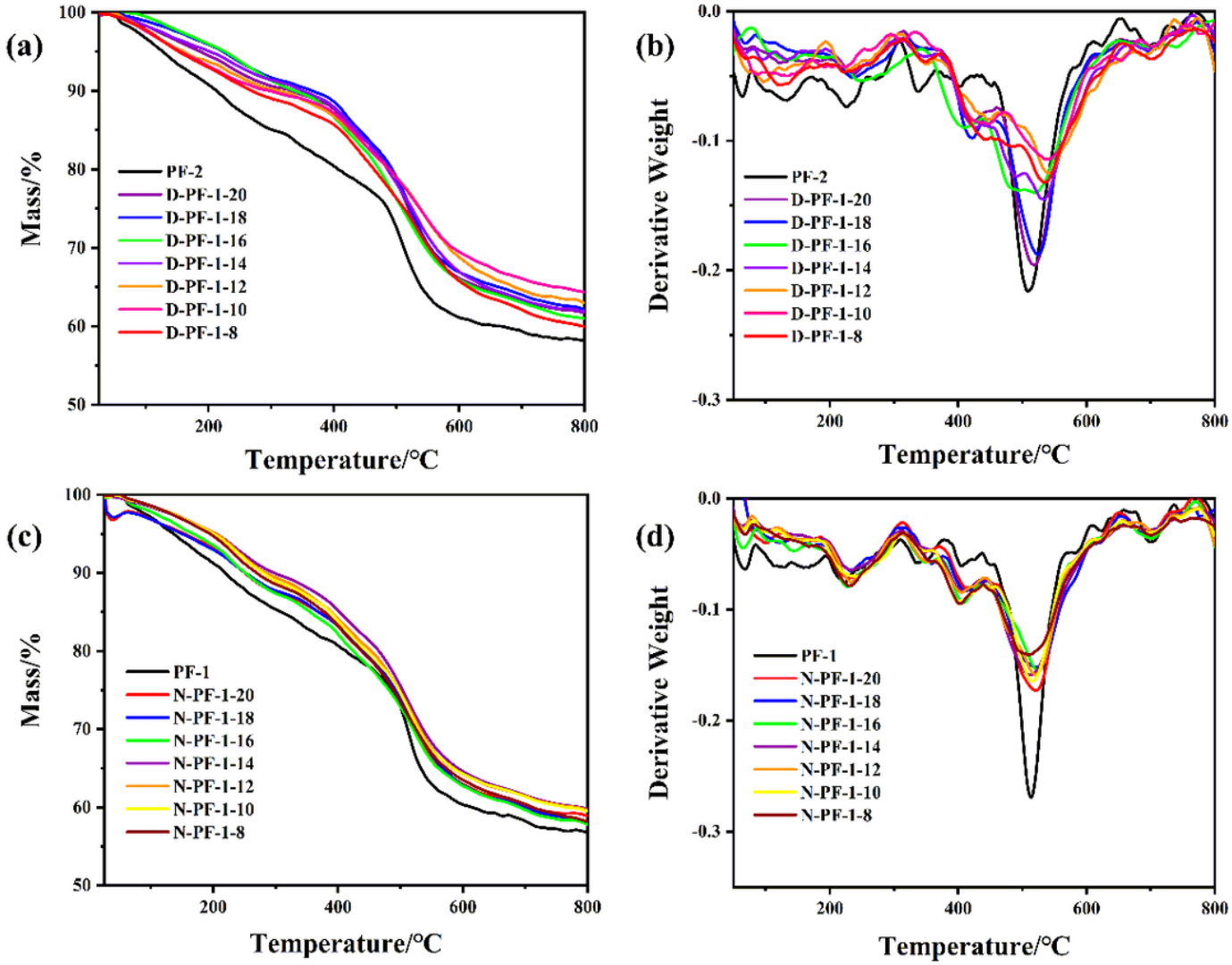

Figure 5

Thermal degradation behavior of resins

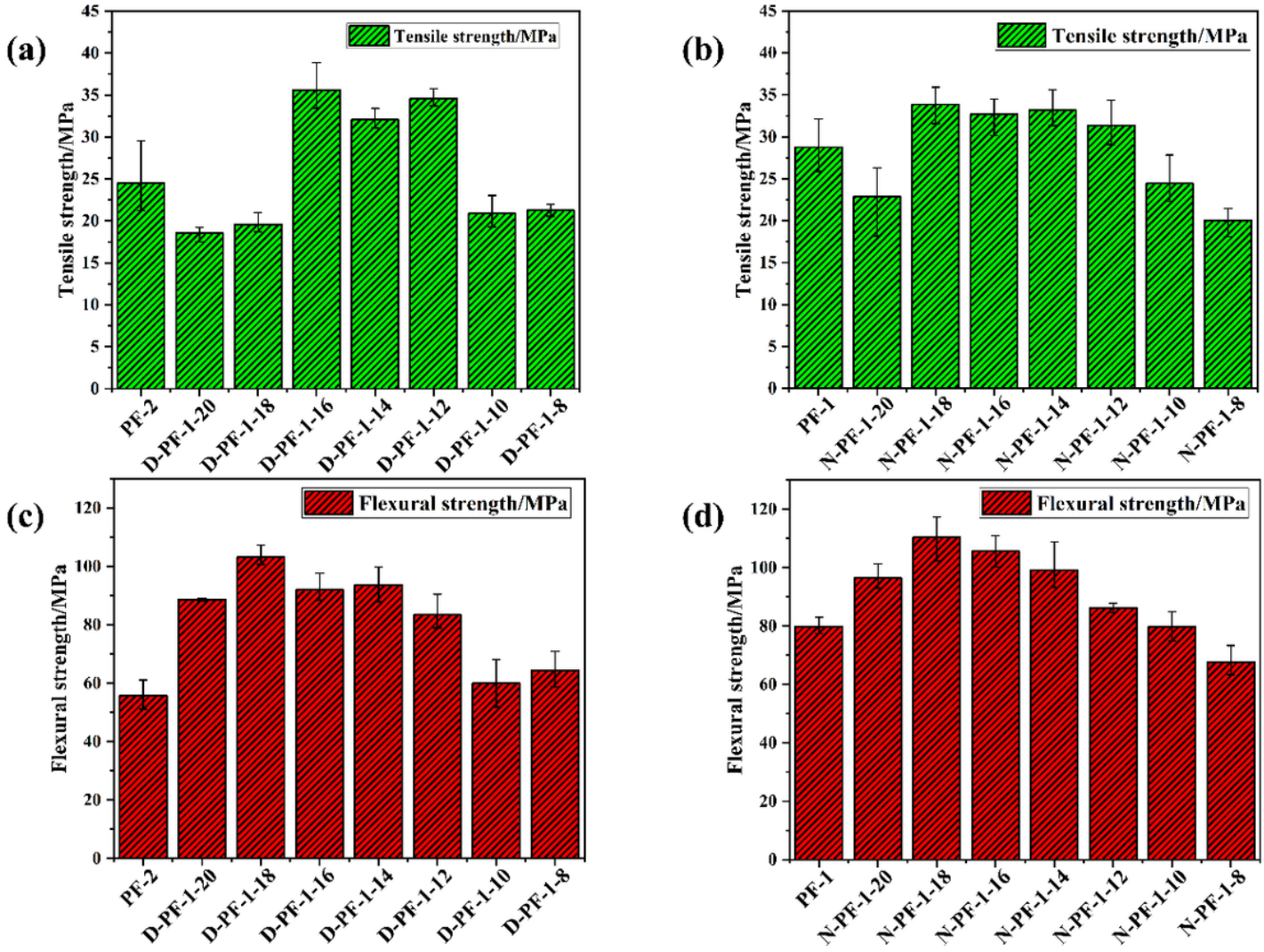

Figure 6

Mechanical properties of resins

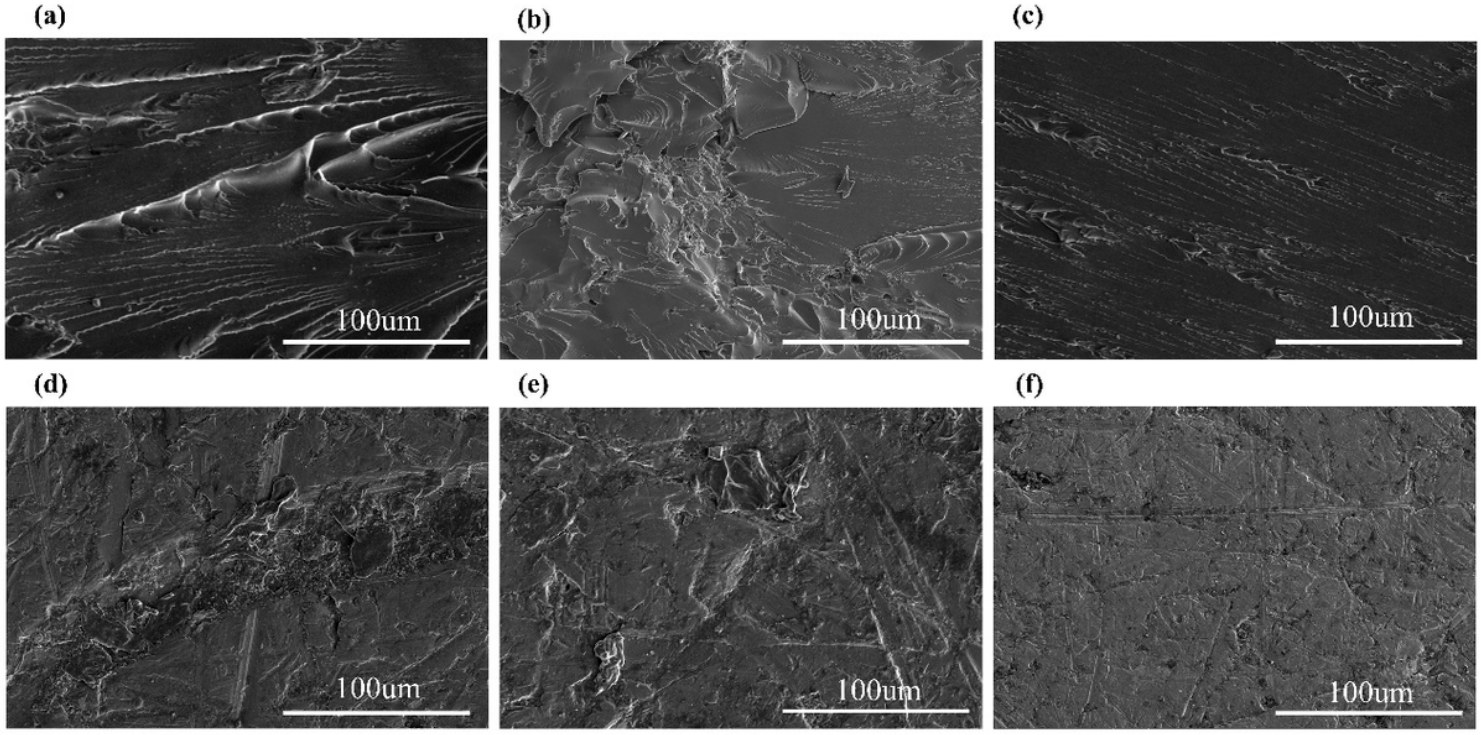

Figure 7

Tensile and flexural fracture surface morphology SEM of resins

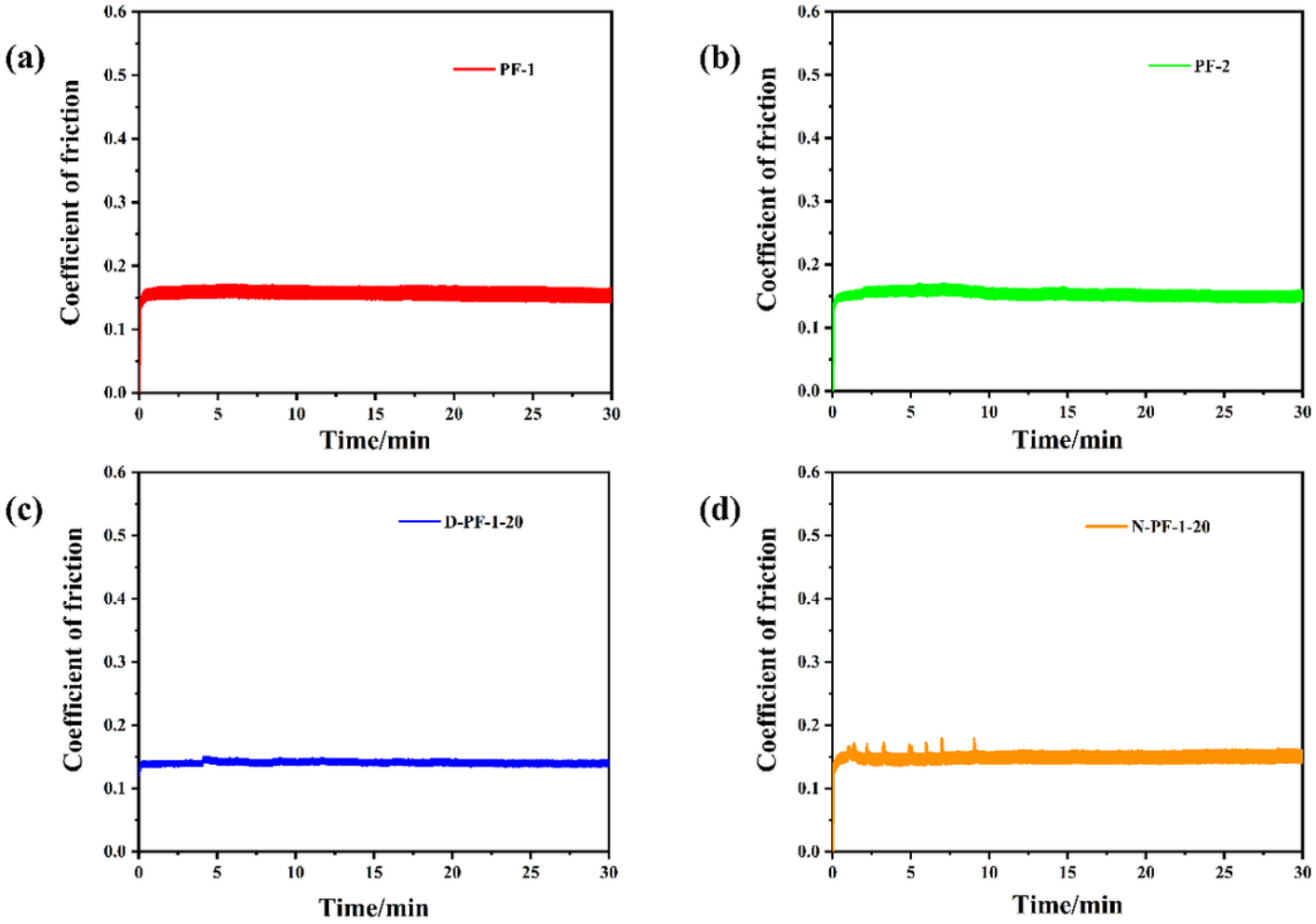

Figure 8

Dynamic coefficient of friction of resins

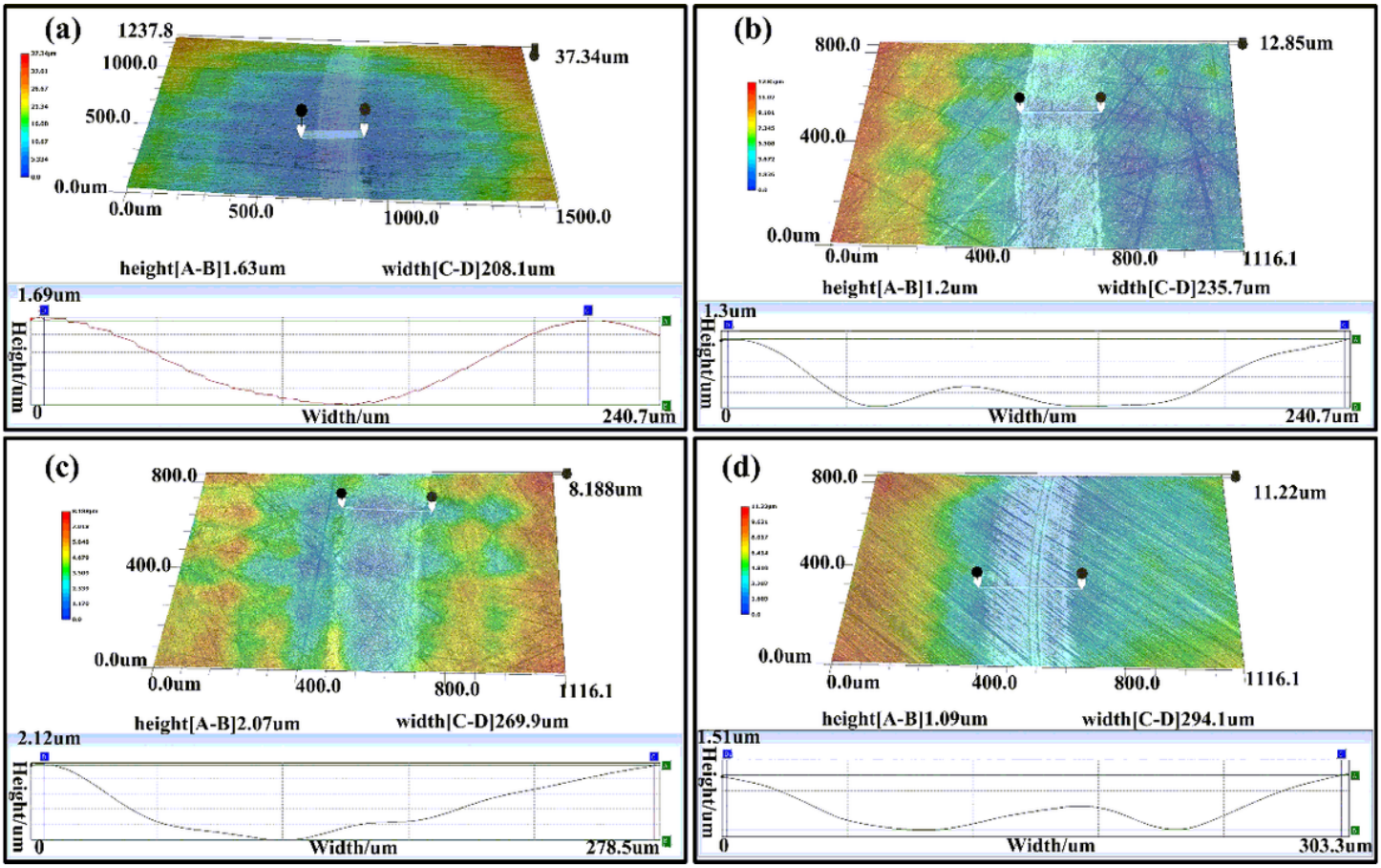

Figure 9

3D profile of resins: (a) D-PF(b)N-PF(c)PF-1(d)PF-2